EE-SSL-1812

EE-SSL-1812

Interim Report

(NASA-CR-120426) SOLAR RADIOMETRY AT MILLIMETER WAVELENGTHS Interim Report (Teledyne Brown Engineering) 30 p HC $4.50 CSCL 03A

N74-32271

Unclas

G3/30 47780

SOLAR RADIOMETRY AT MILLIMETER WAVELENGTHS

May 1974

BROWN ENGINEERING

Cummings Research Park • Huntsville, Alabama 35807

INTERIM REPORT
EE-SSL-1812

SOLAR RADIOMETRY AT MILLIMETER WAVELENGTHS

By

William Henze

May 1974

Prepared For

ELECTROMAGNETIC AND SOLID STATE PHYSICS DIVISION
SPACE SCIENCES LABORATORY
GEORGE C. MARSHALL SPACE FLIGHT CENTER

Contract No. NAS8-26442

Prepared By

RESEARCH LABORATORIES
TELEDYNE BROWN ENGINEERING
HUNTSVILLE, ALABAMA

ABSTRACT

This report covers several areas that were studied during the year, all of which concerned observations that were made or could be made with the radio telescope at the La Posta Astrogeophysical Observatory of the Naval Electronics Laboratory Center in California. In the area of resolution enhancement, the use of Fast Fourier Transform programs was investigated for possible application to millimeter wavelength maps of the Sun. A difficulty that arises with the La Posta maps is that they are limited to 35 arc-minutes square while the smeared out solar image is larger than that.

A list of possible cometary emission lines near 13 millimeters is presented. Although preparation of the list was inspired by the appearance of Comet Kohoutek, the results are applicable to any future comet.

The brightness temperature of the Sun at 8.6 millimeters was measured using the Moon as a calibration source. The result does not confirm a deep absorption feature as apparently observed by earlier workers.

N E Chatterton

N. E. Chatterton, Ph.D.
Manager, Research Laboratories

TABLE OF CONTENTS

1. INTRODUCTION

The acquisition of large quantities of observational data on the Sun from the Apollo Telescope Mount on the Skylab spacecraft and from earlier satellites such as Orbiting Solar Observatory 7 has reemphasized the importance of using combined approaches and methods of observation to study physical phenomena. In other words, data obtained from space should be accompanied by ground-based observations in order to accomplish the best and most broadly based analyses. Because the ATM and OSO experiments involve primarily the ultraviolet and X-ray regions of the spectrum, they are well complemented by ground-based radio observations. The Space Sciences Laboratory at the Marshall Space Flight Center has performed or has had access to such observations in the millimeter wavelength region, and it is important to use these data in studies of the Sun.

Several areas involving radio astronomy of the Sun and other bodies have been pursued and are discussed in this report. These include resolution enhancement of maps of the Sun, possibly detectable line emissions in the millimeter spectral region from comets, and the observation of the brightness temperature of the center of the Sun at 8.6 millimeters and its comparison with models.

2. RESOLUTION ENHANCEMENT

An image can usually be considered to be a convolution of the object with an antenna power pattern or point spread function plus noise. Normally, filtering of noise and deconvolution of the observed image distribution to obtain the true object distribution are accomplished by using Fourier transform techniques. Because the millimeter-wavelength radio maps of the Sun are usually in the form of digitized arrays, we use the finite discrete Fourier transform, whose properties are conveniently summarized by Gentleman and Sande (1966). [We actually use the normalization and some of the conventions given by Brault and White (1971).]

The discrete Fourier transform is given by

$$\tilde{F}(t_k) \equiv N^{-1} \sum_{j=1}^{N} F(x_j) \exp(-i\ 2\pi\ x_j\ t_k) \tag{1}$$

and the inverse by

$$F(x_j) \equiv \sum_{k=1}^{N} \tilde{F}(t_k) \exp(+i\ 2\pi\ x_j\ t_k) \tag{2}$$

where $F(x_j)$ are the data, $x_j = (j - 1)\Delta x$ are the points at which the data are sampled, Δx is the sampling interval, N = the number of data points, and $t_k = (k - 1)/(N\Delta x)$ are the discrete spatial frequencies. Use of the Fast Fourier Transform algorithm, described, for example, by Gentleman and Sande (1966) and by Cochran et al (1967), has significantly reduced the time needed to compute Fourier transforms, thereby making them convenient to use.

The power spectrum is easily computed from the Fourier transform by the relation:

$$P(t_k) = F(t_k)\ F(t_k)^* \tag{3}$$

where $F(t_k)^*$ is the complex conjugate of $F(t_k)$. The power spectrum is a convenient quantity to use in examining the influence of noise on the data. It will be formally used in the optimum filter.

The distribution of intensity or radiance in an image I(x) can usually be written as

$$I(x) = S(x) + N(x) \tag{4}$$

$$= \int_{-\infty}^{\infty} O(x') \ A(x - x') \ dx' + N(x) \tag{5}$$

or in the discrete form

$$I(x_j) = S(x_j) + N(x_j) \tag{6}$$

$$= \sum_{i=1}^{N} O(x_i) \ A(x_j - x_i) + N(x_j) \tag{7}$$

where O(x) is the true object distribution, A(x) is the antenna power pattern or point spread function, N(x) is the noise, and S(x) is the smeared signal which would be observed in the absence of noise. (The two uses of the symbol N should cause no confusion.) The discrete form of the convolution shown in Equation 7 must be considered cyclic, i.e., the N data points repeat themselves. The cyclic property introduced by the sampling process and the finite number of points require care in the restoration process. The two ends of a set of data must smoothly approach the same value.

The attempt to recover the true distribution O(x) form the observed distribution I(x) proceeds as follows. The Fourier transforms of Equations 6 and 7 are

$$\tilde{I}(t_k) = \tilde{S}(t_k) + \tilde{N}(t_k) \tag{8}$$

and

$$\tilde{I}(t_k) = \tilde{O}(t_k) \cdot \tilde{A}(t_k) + \tilde{N}(t_k) \tag{9}$$

where we use the property that the transform of a convolution is equal to the product of the transforms. If we were able to observe $S(x)$, then the solution for $O(x)$ would simply be the inverse transform of $\tilde{O}(t)$ given by

$$\tilde{O}(t) = \tilde{S}(t)/\tilde{A}(t) \quad . \tag{10}$$

This process is limited only by the fact that $\tilde{A}(t)$ must normally not be zero. If we let

$$R_0(t) = \begin{cases} \tilde{S}(t)/\tilde{A}(t) , & \tilde{A}(t) \neq 0 \\ 0 , & \tilde{A}(t) = 0 \end{cases} \tag{11}$$

then $R_0(x)$ is known as the principal solution (Bracewell and Roberts, 1954). Normally $\tilde{A}(t)$ will be zero beyond some frequency corresponding to the Rayleigh limit. In the presence of noise, the simple application of the restoration process to the image yields

$$\tilde{R}_1(t) = \tilde{I}(t)/\tilde{A}(t) \tag{12}$$

$$= \tilde{S}(t)/\tilde{A}(t) + \tilde{N}(t)/\tilde{A}(t) \tag{13}$$

$$= \tilde{O}(t) + \tilde{N}(t)/\tilde{A}(t) \quad . \tag{14}$$

(Again, we have to be careful about $\tilde{A}$ being zero.) Because $\tilde{A}(t)$ becomes small at high frequencies, Equation 14 amplifies the high-frequency noise with disastrous effects on the restoration. To avoid the amplification of the noise, an optimum filter is applied (Brault and White, 1971):

$$\tilde{R}_2(t) = \frac{\tilde{I}(t)}{\tilde{A}(t)} \cdot \frac{P_S(t)}{P_S(t) + P_N(t)} \tag{15}$$

where $P_s(t)$ and $P_N(t)$ are the power spectra of the smeared signal and the noise. These power spectra can often be modeled after examination of the power spectrum of the image. Usually P_N can be considered to be a constant equal to the mean of its high-frequency component. In other words, all of the high-frequency components of the observed image are noise, and the noise power spectrum is independent of frequency.

The development described above will not allow recovery of the object distribution at frequencies above that corresponding to the minimum separation given by the Rayleigh criterion. In recent years, there has been considerable effort devoted to attempts at resolution beyond the Rayleigh limit. Several schemes have been devised to extrapolate the spectra to higher frequencies. These schemes are based on various properties, such as the fact that the true object distribution must be positive or that it has a finite extent. However, it has been shown, e.g., by Rushforth and Harris (1968) and Miller (1972) that the methods based on the finite extent of the object are severely limited by noise. The signal-to-noise ratio required to improve even slightly on the Rayleigh limit is extremely high; thus, the Rayleigh criterion represents a practical limit to what can be realized at reasonable signal-to-noise ratios.

This discussion has been given in terms of one-dimensional distributions. Extension of two dimensions is usually straightforward.

The application of restoration techniques to the 8.6-millimeter maps of the Sun obtained at La Posta is subject to several limitations. The presence of noise will cause difficulties. One of the main sources of noise is the variation of the transmission of the Earth's atmosphere during the time required to make a complete map (about one hour). Another limitation is due to the truncated size of the maps. They normally cover a solid angle about 35 arc-minutes square, whereas the Sun is 32 arc-minutes in diameter and the antenna pattern has a half-power width of several arc-minutes. Use of the Fast Fourier Transform on the sharply cutoff image would create false high-frequency components in the transform (aliasing). A possible way around this problem would be to artifically extrapolate the image according to a known mean distribution. Of course, no details near the limb of the Sun would then be recoverable.

3. LINE EMISSION FROM COMETS

The discovery of Comet Kohoutek more than nine months before its perihelion passage in late December 1973 made it possible for observers to have considerable time to prepare special equipment and to plan observing programs. At that time it appeared that support might be available to build a line receiver to be used on the 60-foot antenna at the La Posta Observatory of the Naval Electronics Laboratory Center near San Diego, California. Because it would be desirable to search for line emission from comets, especially from certain molecules, an effort was made to identify which lines might be detected. Before listing the possible lines, we present a brief summary of the characteristics of comets, based in part on the review by Brandt (1968) and the proceedings of the Tucson Comet Conference (Kuiper and Roemer, 1972).

3.1 PHYSICAL CHARACTERISTICS OF TYPICAL COMETS

Comets are usually described as having three parts: a solid nucleus, a coma of dust and neutral molecules, and a tail of ionized molecules or dust.

The nucleus is thought to be 1 to 10 kilometers in radius and composed of an "icy conglomerate" (Whipple, 1963) containing frozen compounds such as H_2O, NH_3, CH_4, CO_2, C_2N_2, etc. Embedded in the icy material is meteoric material. The mass may be on the order of 10^{16} to 10^{21} grams. The nucleus has never been directly observed.

The ices in the nucleus presumably sublimate in vacuum at temperatures on the order of several hundred degrees Kelvin and dissociate to form the simpler daughter molecules which are observed in the coma. The parent or precursor molecules themselves, such as H_2O, NH_3, and CH_4, have not been observed but are inferred from the existence of the observed daughter molecules such as the radicals OH, CH, NH, and NH_2. Because the parent molecules have not been observed, it is, therefore, important to search for them in order to better understand the chemistry of comets. The radius of the coma is typically about 10^5 kilometers, corresponding to more than 2 arc-minutes at a distance of one astronomical unit. Therefore, the coma would make a suitable target for observation in the millimeter range by the La Posta radio telescope. However, the parent molecules would probably exist only in a much smaller volume of the coma surrounding the nucleus. Typical expansion velocities of molecules ejected from the nucleus are on the order of 1 km/sec. Because the total gas density is low, ranging from about 10^{12} to 10^{14} molecules/cm^3 near the nucleus to 10^2 to 10^4 molecules/cm^3 at the outer boundary, association processes are not important. In other words, once the parent molecules are dissociated, the daughter components remain apart and never recombine to form the parent. Dust and metallic atoms are also observed in the coma. A fairly recent development has been the observation of a hydrogen Lyman-α halo which extends out to a radius of about 10^6 kilometers.

The third major element of a comet is the tail, reaching up to 10^8 kilometers or one astronomical unit in length. There are two types of tails; occasionally both types appear in the same comet. Type I tails are composed of ionized molecules and atoms with some neutral atoms and are straight, pointing, to a first approximation, away from the Sun. Type II tails are strongly curved and are composed of dust showing a reflected solar spectrum.

In the visible spectrum and for hydrogen Lyman-α, the predominant excitation mechanism is resonance fluorescence by sunlight. In the case of the forbidden oxygen line, the atom is presumably formed in the excited state during the photo-dissociation of its parent molecule. It is not known what the excitation mechanism for microwave lines would be -- radiative, collisional, or excitation -- during the formation or release of the molecule. Relative populations of levels emitting the observed lines could show how the levels are excited. If they are collisionally excited, densities or limits on densities may be inferred.

3.2 OBSERVATIONAL POSSIBILITIES

The spectral region around 13 millimeters appeared to have several lines of interest, and as there would not have been any technical difficulty in building a receiver for that wavelength, only lines in that spectral region were considered. Table 1 contains a list of lines near 13 millimeters which might be observed in comets. Most of the information on molecular lines is based on the Microwave Spectral Tables (National Bureau of Standards Monograph No. 70). After the information was compiled, it was discovered that Huebner (1970) had made a more complete listing.

Also shown in the table are some hydrogen and helium lines taken from Lilley and Palmer (1968). These lines are known as recombination lines because they normally are emitted following recombination of an ion with an electron. Because the densities are so low, recombination is likely to be rare and the lines are probably too weak to be observed.

The coma would provide the best location to search for line emissions.

Unfortunately, no financial support became available to enable observations to be made of Comet Kohoutek. However, it will still be desirable to search for line emissions in the microwave spectra of future comets.

TABLE 1. MICROWAVE LINES WHICH MIGHT BE OBSERVED IN COMETS

MOLECULE OR ATOM	TYPE OF LINE	TRANSITION	FREQUENCY (MHz)	REMARKS
H_2O (Water)	Rotational	$5_{23} - 6_{16}$	22235.22	Levels are 446 cm^{-1} above ground state (equivalent to 22.4 μm).
NH_3 (Ammonia)	Inversion Doublet	(1, 1) (2, 1) (2, 2) (3, 2) (3, 3) (4, 4) (6, 6) (5, 5) (4, 3)	23694.49 23098.78 23722.63 22834.17 23870.13 24139.41 25056.02 24532.98 22688.29	(6, 6) level is almost 300 cm^{-1} above ground state; others are all lower. All but last two transitions have been observed in interstellar medium.
OH (Hydroxyl)	Lambda Doubling	$^2\Pi_{3/2}$ 9/2, 4 F' = 4 F" = 5 4 4 5 5 5 4	 23806.5 23818.18 23826.90 23837.8	Levels are about 375 cm^{-1} above ground state.
NH		$F_2(J = 1)-F_1(J = 2)$	25586.4	Predicted by Kerns and Duncan 1972.
HNCO (Isocyanic Acid)		$0_{00} - 1_{01}$	21982.	
CH_3OH (Methylalcohol)		(J, K) = 4, 1-4, 2 5, 1-5, 2 6, 1-6, 2 7, 1-7, 2 8, 1-8, 2	24933. 24959. 25018. 25125. 25294.	
H (Hydrogen)	Recombination	66α 65α 64α 63α	22364.17 23404.28 24509.91 25686.28	
He (Helium)	Recombination	66α 65α 64α 63α	22373.28 23413.82 24519.89 25696.75	

4. SOLAR BRIGHTNESS TEMPERATURE AT 8.6 MILLIMETERS

Several reviews of the solar millimeter spectrum (e.g., Linsky, 1973; Kislyakov, 1970; Shimabukuro and Stacey, 1968) have indicated the presence of an absorption feature or depression in the solar spectrum in the vicinity of 6 to 9 millimeters. Because such a feature is not expected according to our present understanding of the solar atmosphere, it is important to verify its existence. We therefore decided to remeasure the brightness temperature of the Sun by carefully determining the ratio of the brightness of the Sun and Moon and using the Moon as a standard source. This section of the report reviews the background for the reasoning behind the measurement, describes the computation of the topocentric coordinates of the Moon which were needed, and gives our results in which we did not confirm the presence of a deep absorption feature. A report on our work, which was carried out jointly with Max Bleiweiss of the Naval Electronics Laboratory Center and Fred Wefer of the Megatek Corporation, was presented at the meeting of the Solar Physics Division of the American Astronomical Society held in Honolulu, Hawaii, in January 1974. The abstract of the paper is reproduced in Appendix A.

4.1 BACKGROUND

Most models of the solar chromosphere, whether of one or more components, have the temperature increasing outward. Therefore, as one observes at longer and longer wavelengths in the millimeter region, corresponding to higher opacities, one should see a monotonically increasing brightness temperature. However, many reviews of the solar millimeter spectrum show a depression or absorption feature. For example, Shimabukuro and Stacey (1968) and Kislyakov (1970) plot many observations which have considerable scatter but appear to have a minimum near 6 millimeters. The exact position (and possibly even the existence) of the minimum is poorly defined because of the scatter. On the other hand, Linsky (1973) has accepted only those measurements made relative to the Moon and has recalibrated them using his own review of the lunar spectrum. His plot, which is shown in Figure 1, shows a depression of over 2000°K at the two data points at 8 and 8.6 millimeters. The observation at 8.6 millimeters by Ulich, Cogdell, and Davis (1973) is claimed by them to have been verified in unpublished work by Ulich. Published explanations that have been offered for the minimum include a multicomponent atmosphere with the relative volume of hot material decreasing with height (Zheleznyakov, 1964) and scattering of the radio waves by plasma-turbulence waves (Kaplan and Tsytovich, 1967).

In view of the importance of irregularities in the millimeter spectrum to understanding the details of chromospheric structure, it was decided that the existence of the minimum should be verified by a measurement at La Posta of the brightness temperature at 8.6 millimeters.

4.2 TOPOCENTRIC COORDINATES OF THE MOON

Because the Moon would be used as a standard calibration source, it was necessary to be able to point the La Posta radio telescope accurately at the center of the Moon. Computer programs already existed at La Posta to use astronomical positions as tabulated in the American Ephemeris and Nautical Almanac. The tabulated positions are relative to the center of the Earth. The Moon, however, is so close to the Earth that parallax affects its apparent position as seen by an observer at an arbitrary point on the surface of the Earth. Therefore, it was necessary to write a computer program to convert from geocentric to topocentric coordinates.

The relationships between the geocentric and topocentric coordinates are summarized below with the particular form and notation taken from Raine (1970). The topocentric hour angle h_T and declination δ_T are given by

$$\sin h_T = A/S \tag{16}$$

$$\cos h_T = B/S \tag{17}$$

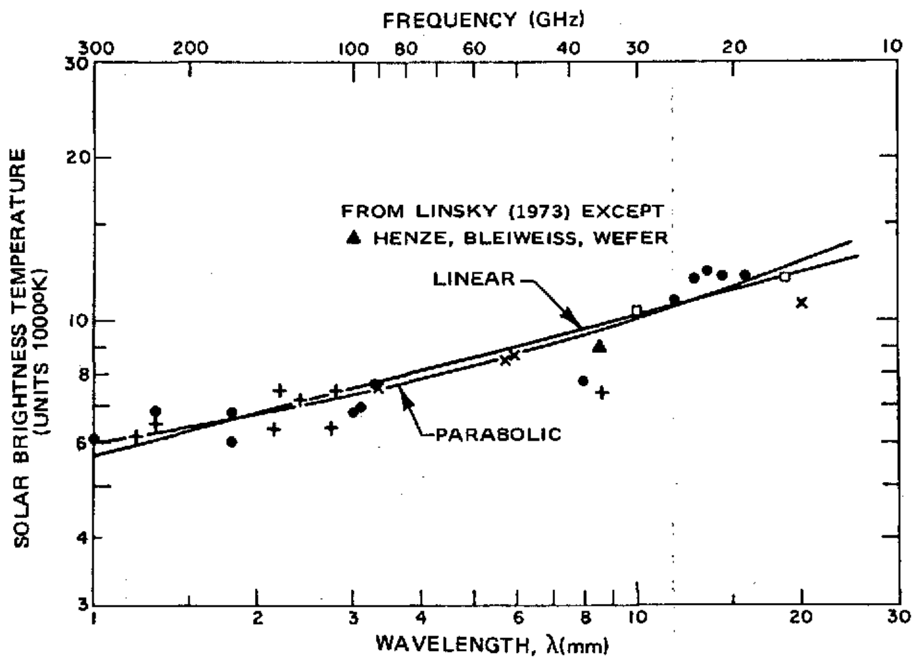

FIGURE 1. OBSERVED SOLAR MILLIMETER SPECTRUM. Points and fitted curves taken from Linsky (1973) except for ▲ from this investigation.

and

$$\sin \delta_T = C/F \tag{18}$$

where

$$A = \cos \delta_G \sin h_G \tag{19}$$

$$B = \cos \delta_G \cos h_G - \rho \cos \phi' \sin \Pi_G \tag{20}$$

$$C = \sin \delta_G - \rho \sin \phi' \sin \Pi_G \tag{21}$$

$$D = A^2 + B^2 \tag{22}$$

$$F = (D + C^2)^{1/2} \tag{23}$$

and the geocentric hour angle h_G is given by

$$h_G = ST_0 + 1.00273791\ t - \lambda - \alpha_G \quad . \tag{24}$$

The geocentric right ascension α_G, geocentric declination δ_G, and horizontal parallax of the Moon Π_G are tabulated; also tabulated is ST_0, the Greenwich sidereal time at 0 hours Universal Time (U.T.). λ is the longitude, ρ is the distance from the center of the Earth in equatorial Earth radii, and ϕ' is the geocentric latitude of the observer. t is the Universal Time and 1.00273791 t is the sidereal time elapsed since 0 hours U.T.

Also convenient for the La Posta observers are the hour angles from the Greenwich meridian:

$$h_{T,Grw} = h_T + \lambda \tag{25}$$

and the topocentric right ascension:

$$\alpha_T = ST_0 + 1.00273791\ t - \lambda - h_T \quad . \tag{26}$$

The La Posta position is specified by

$\lambda = 116^\circ\!.4512$

$\rho = 0.99902436$

$\phi' = 32^\circ\ 30'\ 7''\!.925$.

A copy of the computer program is contained in Appendix B. Because the observations were to be made in October 1973, certain parts of the program were written with that knowledge incorporated. Use of the program for a different time would require slight modifications. The input data needed, which are all found in the American Ephemeris and Nautical Almanac, are the Greenwich sidereal time at 0 hours U.T. for each day and the geocentric right ascension, geocentric declination, and horizontal parallax of the Moon for each hour.

4.3 OBSERVATIONAL RESULTS

The observations of the Sun and Moon were obtained with the 60-foot (18.3-meter) diameter radiotelescope at the La Posta Astrogeophysical Observatory of the Naval Electronics Laboratory Center near San Diego on 26 October 1973. Preliminary measurements were made on 24 October but were not used in the final results. The date was chosen to be near new moon so that the Sun and Moon would be close together in the sky, minimizing differential atmospheric effects. The Moon was used as a standard source, following Linsky's (1973) suggestion. Measurements were made at 8.6 millimeters (35 GHz), at which wavelength the antenna has a half-power beamwidth of 2.8 arc-minutes. There was no solar activity present near the center of the Sun.

Two types of observations were made: analog drift scans across an entire solar or lunar diameter and digitized small maps of the central regions of the disks. The maps normally consisted of 5 x 5 arrays with a grid spacing of 1 arc-minute. Table 2 lists some information about the scans and maps. Because of the ease of their use in quantitative work, only maps, particularly one map each of the Sun and Moon, were used in the final results.

The observational process included a measurement of the brightness temperature of the sky nearby and at the same elevation as the Sun or Moon. The sky temperature was subtracted off in the reduction of the data. Internal calibration was carried out by the use of a 3000°K noise tube and a 375°K oven.

TABLE 2. TIMES AND POINTING INFORMATION ON DRIFT SCANS AND MAPS
26 OCTOBER 1973

SOURCE	TIME (Universal Time)	AZIMUTH (deg)	ELEVATION (deg)
Drift Scans			
Sun	1835	161.1	42.7
Moon	1912	167.3	36.8
Moon	2200	213.2	30.0
Sun	2221	229.5	29.8
Maps			
Sun*	~1710		~30.0
Moon	1924	170.7	37.2
Sun	2130	217.6	36.2
Moon	2142	209.1	31.8
Sun	2232	232.0	26.8

*Taken from center of large map on the entire Sun.

Because of the ease of their use in quantitative work, only the reduced observations from the maps are presented here. The results in units of antenna temperature are shown in Table 3. The source temperature is the mean of the 25 or 21 individual data points with the sky already removed. The rms deviation σ is effectively equal to the standard deviation of a single measurement from the mean; it has not been reduced by the square root of the number of points.

The two maps which were ultimately used were selected because they were taken most closely together in time -- the solar map at 2130 U.T. and the lunar map at 2142 U.T. A flaw in the computerized data recording process limited the solar map to 21 points instead of 25. The Sun-to-Moon ratio is then

TABLE 3. ANTENNA TEMPERATURES FROM MAPS
26 OCTOBER 1973

SOURCE	TIME (Universal Time)	NUMBER OF DATA POINTS	ANTENNA TEMPERATURE (°K)		
			SKY	SOURCE (Sky Removed)	σ = rms DEV.
Sun	~1710	25		4296	23.1
Moon	1924	25	15.9	102.2	1.75
Sun	2130	21	14.1	4376	25.8
Moon	2142	25	16.7	104.9	1.76
Sun	2232	25	26.0	4335	19.1

$$\frac{T_S}{T_M} = \frac{4376}{104.9} = 41.72 \quad . \tag{27}$$

If the brightness temperature of the new moon is taken to be 219°K (Linsky, 1973), then the ratio of brightness temperature to antenna temperature is

$$\frac{T_B}{T_A} = \frac{219}{104.9} = 2.088 \quad . \tag{28}$$

The solar brightness temperature is then 9140°K, and the measured rms brightness temperature deviations are σ_S = 53.9°K and σ_M = 3.67°K. To arrive at an uncertainty combining both the solar and lunar measurement uncertainty, we use the expression

$$\sigma = \left[\sigma_S{}^2 + \left(\frac{T_S}{T_M} \sigma_M \right)^2 \right]^{1/2} \tag{29}$$

to obtain σ = 162°K.

The final result for the brightness temperature of the center of the solar disk is then

$$T_B = 9140 \pm 160°K \quad .$$

The uncertainty is a statistical measure equal to the combination of the rms deviations of both the solar and lunar measurements. Of course, there are additional sources of error arising from the effects of the Earth's atmosphere, weak activity on the Sun, and irregularities in the surface brightness near the center of the Moon.

Our result is shown as the triangular shaped point in Figure 1 where it may be compared with Linsky's (1973) fitted curves -- 9641°K at 8.6 millimeters from the parabolic curve -- and with the observed point shown as a cross by Ulich, et al (1973) -- 7410°K as recalibrated by Linsky. Although the point is still below the curves that Linsky fitted to the data, it clearly does not confirm a deep depression. Our measurement is also shown in Figure 2 where, along with Linsky's curve, it is compared to predictions of two recent models -- the Harvard-Smithsonian Reference Atmosphere [Gingerich, et al (1971)] and a model by Vernazza and Noyes (1972). It is notable that, especially at longer wavelengths, Linsky's curve is significantly higher than the model predictions.

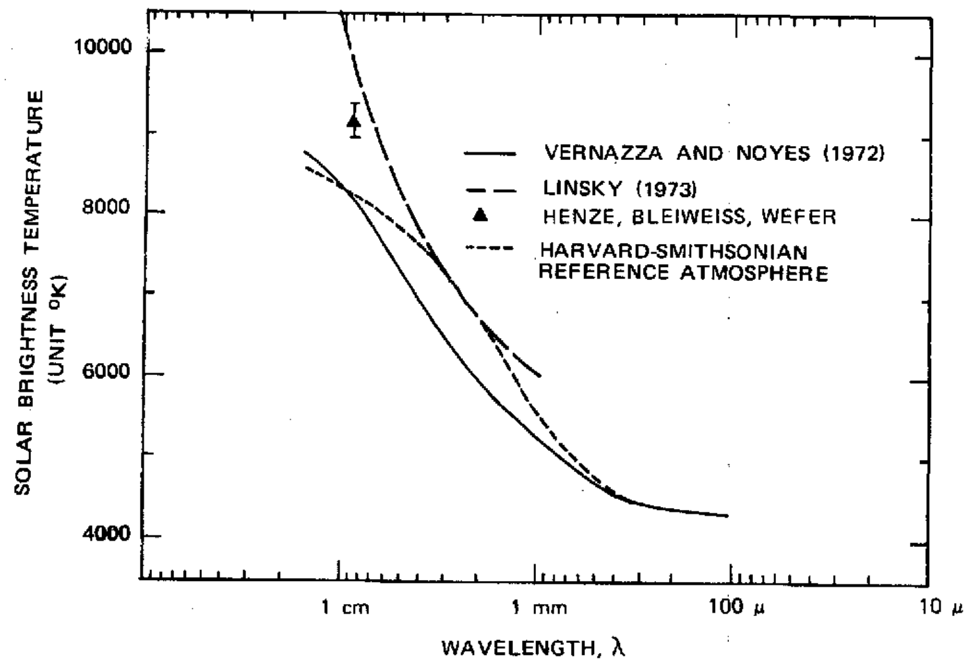

FIGURE 2. SOLAR MILLIMETER SPECTRUM

APPENDIX A. ABSTRACT OF PRESENTATION

The abstract of presentation at the meeting of the Solar Physics Division of the American Astronomical Society held in Honolulu, Hawaii, in January 1974 is presented below. The abstract was published in the Bulletin of the American Astronomical Society, Vol. 6, No. 2, Part II, p. 288.

Brightness Temperature of the Sun at 8.6 Millimeters - Presence of an Absorption Feature? W. HENZE, Teledyne Brown Engineering, M. BLEIWEISS, Naval Electronics Lab. Center, & F. WEFER, Megatek Corp. - Reviews of the solar spectrum at millimeter wavelengths (J. L. Linsky, 1973, Solar Phys. 28, 409; A. G. Kislyakov, 1971, Soviet Phys. Uspekhi 13, 495) together with recent work by B. T. Ulich (U. Texas, unpublished) indicate the presence of a depression or absorption feature near 8 mm wavelength. Because such a feature is not expected according to our present understanding of the solar atmosphere, it is important to verify the existence of the feature. Therefore, we have observed the brightness temperature of the center of the solar disk relative to the center of the new moon at 8.6 mm with the 60 ft antenna of the Naval Electronics Laboratory Center at La Posta, California. Our preliminary results based on the temperature of the new moon given by Linsky (op. cit.) do not confirm the presence of a deep absorption feature or depression near 8 mm.

APPENDIX B. COMPUTER PROGRAM USED TO COMPUTE TOPOCENTRIC COORDINATES OF THE MOON

```
C      PROGRAM TPCORD
C    W. HENZE     OCTOBER 1973     TBE
C   COMPUTES TOPOCENTRIC COORDINATES OF LUNAR CENTER
      DIMENSION IDYSID(15),SDTGT(15),IDYMN(126),IHRUT(126),HAT(126)
     1,HATG(126),DCT(126),RAT(126)
      RHSNPP = .53680777
      RHCSPP = .842547975
      PI = 3.1415926536
      XLONG = 2.032456858
C...XLONG = LONGITUDE IN RADIANS
      WRITE(6,212)
  212 FORMAT(1H1,39HSIDEREAL TIME AT GREENWICH AT 0 HR U.T.//1H ,
     1 7HOCTOBER/1H ,5H DAY,5X,27HHOUR  MIN  SECOND   RADIANS)
      DO 1 I=1,15
      READ(5,111) IDYSID(I),IHST,MST,SST
  111 FORMAT(I3,I4,I3,F7.3)
      HST = IHST
      XMST = MST
      SDTG = HST +(XMST+SST/60.)/60.
      SDTGT(I) = SDTG*(PI/12.)
C...SDTGT = SIDEREAL TIME AT GREENWICH AT 0 HR U.T. IN RADIANS
      WRITE(6,211) IDYSID(I),IHST,MST,SST,SDTGT(I)
  211 FORMAT(1H ,I5,I8,I6,F8.3,F10.5)
    1 CONTINUE
      WRITE(6,213)
  213 FORMAT(1H1,109H ST MN UT PDT  GEOCENT RIGHT ASCNSN  GEOCENT DECLINATION
     1ATION  HORZNTL PARALLAX    TOP DEC TOPO HA TOPO HA TOPO RA/1H ,
     2 107H DY DY HR HR   HR MN  SEC     RAD      DG AM ARCSC  RAD     AM
     3ARCSC  RAD          RAD  LOC.RAD GRW.RAD   RAD)
      DO 2 J=1,126
      READ(5,112) IDYMN(J),IHRUT(J),IRAHG,IRAMG,RASG,IDCDG,IDCMG,DCSG
     1,IPRMG,PRSG
  112 FORMAT(I3,I3,I4,I3,F7.3,I4,I3,F6.2,I4,F6.2)
      HRUT = IHRUT(J)
      RAHG = IRAHG
```

```
      RAMG = IRAMG
      DCDG = IDCDG
      DCMG = IDCMG
      PRMG = IPRMG
      RA = RAHG+(RAMG+RASG/60.)/60.
      RAG = RA*(PI/12.)
C...RAG = GEOCENTRIC RIGHT ASCENSION OF MOON IN RADIANS
      IDSN = 1
      IF(J-30) 7,11,11
   11 IDSN = -1
      DCDG = -DCDG
    7 DEC = DCDG+(DCMG+DCSG/60.)/60.
      IF(IDSN) 8,9,9
    8 DEC = -DEC
    9 DCG = DEC*(PI/180.)
C...DCG = GEOCENTRIC DECLINATION OF MOON IN RADIANS
      PR = PRMG+PRSG/60.
      PRG = PR*(PI/10800.)
C...PRG= HORIZONTAL PARALLAX IN RADIANS
      TR = 1.00273791*HRUT   *(PI/12.)
```



```
      ID = J+8
      ID = ID/9
      SDG = SDTGT(ID)+TR
C...SDG = PRESENT GREENWICH SIDEREAL TIME
      HAG = SDG-XLONG-RAG
      SNPRG = SIN(PRG)
      CSDCG = COS(DCG)
      SNDCG = SIN(DCG)
      SNHAG = SIN(HAG)
      CSHAG = COS(HAG)
      A = CSDCG*SNHAG
      B = CSDCG*CSHAG-SNPRG*RHCSPP
      C = SNDCG-SNPRG*RHSNPP
      D = A*A+B*B
```

```
      S = SQRT(D)
      F = SQRT(D+C*C)
      SNDCT = C/F
      DCT(J) = ARSIN(SNDCT)                                     IBM 7094
C...DCT = TOPOCENTRIC DECLINATION IN RADIANS
      SNHT = A/S
      CSHT = B/S
      HT = ARSIN(SNHT)                                          IBM 7094
      IF(CSHT)4,5,5
    4 HT = PI-HT
      IF(SNHT) 12,5,5
   12 HT = HT-2.*PI
    5 HAT(J) = HT
C...HAT = LOCAL TOPOCENTRIC HOUR ANGLE IN RADIANS
      HATG(J) = HAT(J)+XLONG
C...HATG = GREENWICH TOPOCENTRIC HOUR ANGLE IN RADIANS
      IPDT = IHRUT(J)-7
      RAT(J) = SDG-HATG(J)
C...RAT = TOPOCENTRIC RIGHT ASCENSION IN RADIANS
      WRITE(6,214) IDYSID(IC),IDYMN(J),IHRUT(J),IPDT,IRAHG,IRAMG,RASG
     1,RAG,IDCDG,IDCMG,DCSG,DCG,IPRMG,PRSG,PRG,DCT(J),HAT(J),HATG(J),
     2RAT(J)
  214 FORMAT(1H ,4I3,1X,I4,I3,F7.3,F8.5,I4,I3,F6.2,F8.5,I4,
     1 F6.2,F8.5,3X,4F8.5)
    2 CONTINUE
      WRITE(6,215)
  215 FORMAT(1H1,20X,4(3X,11HTOPOCENTRIC)/1H ,75HOCTOBER    UT    PDT
     1DECLINATION   HOUR ANGLE    DECLINATION   HOUR ANGLE/1H ,74H  DAY
     2    HOUR  HOUR    DEG   MIN     DEG   MIN      DEGREES        DEGRE
     3ES)
      DO 3 J=1,126
      DCD = DCT(J)*(180./PI)
      DEC = DCD
      IF(DCD) 13,14,14
   13 DEC = -DEC
   14 IDDG = DEC
      XIDDG = IDDG
      XDMN = (DEC-XIDDG)*60.
      IF(DCD) 15,16,16
   15 IF(IDDG) 17,17,18
   17 IDDG = -0
      GO TO 16
```

```
 18 IDDG = -IDDG
 16 CONTINUE
    HTD = HATG(J)*(180./PI)
    HT = HTD
    IF(HTD) 19,20,20
 19 HT = -HT
 20 IHAD = HT
    XIHAD = IHAD
    XHMN = (HT-XIHAD)*60.
    IF(HTD) 21,22,22
 21 IF(IHAD) 23,23,24
 23 IHAD =-0
    GO TO 22
 24 IHAD = -IHAD
 22 CONTINUE
    IPDT = IHROT(J)-7
    WRITE(6,216) IDYMN(J),IHROT(J),IPDT,IDDG,XDMN,IHAD,XHMN,DCD,HTD
216 FORMAT(1H ,I5,I8,I6,I8,F7.2,I7,F7.2,F12.4,F14.4)
  3 CONTINUE
    STOP
    END
```

BIBLIOGRAPHY

Bracewell, R. N., and Roberts, J. A., 1954: "Aerial Smoothing in Radio Astronomy", Australian J. Phys. 7, 615.

Brandt, J. C., 1968: "The Physics of Comet Tails", Annual Rev. Astron. and Astrophys. 6, 267.

Brault, J. W., and White, O. R., 1971: "The Analysis and Restoration of Astronomical Data via the Fast Fourier Transform", Astron. Astrophys. 13, 169.

Cochran, W. T., Cooley, J. W., Favin, D. L., Helms, H. D., Kaenel, R. A., Lang, W. W., Maling, G. C., Nelson, D. E., Rader, C. M., and Welch, P.D., 1967: "What Is the Fast Fourier Transform?", IEEE Trans. on Audio and Electroacoustics AU-15, 45, and Proc. IEEE 55, 1664.

Gentleman, W. M., and Sande, G., 1966: "Fast Fourier Transforms for Fun and Profit", Proceedings of the 1966 Fall Joint Computer Conference, American Federation of Information Processing Societies, Vol. 29, p. 563.

Gingerich, O., Noyes, R. W., Kalkofen, W., and Cuny, Y., 1971: "The Harvard-Smithsonian Reference Atmosphere", Solar Phys. 18, 347.

Huebner, W. F., 1970: "A Proposal for the Detection of Mother Molecules in Comets by Their Microwave Lines", Los Alamos Scientific Laboratory Report No. LA-4542-MS.

Kaplan, S. A., and Tsytovich, V. N., 1967: "An Interpretation of the Dip in the Spectrum of Millimeter Solar Radio Emission", Astronomicheskii Zhurnal 44, 1036; translated in Soviet Astronomy-AJ 11, 834 (1968).

Kerns, B., and Duncan, A. B. F., 1971: "Predictions on Finding the NH and NH_2 Radicals in Interstellar Space", Astrophys. J. 172, 331.

Kislyakov, A. G., 1970: "Radioastronomical Investigations in the Millimeter and Submillimeter Bands", Uspekhi Fiz. Nauk 101, 607; translated in Soviet Physics Uspekhi 13, 495 (1971).

Kuiper, G. P., and Roemer, E. (editors), 1972: Comets: Scientific Data and Missions, Proceedings of the Tucson Comet Conference, April 1970; Lunar and Planetary Laboratory, University of Arizona.

Lilley, A. E., and Palmer, P., 1968: "Tables of Radio-Frequency Recombination Lines", Astrophys. J. Suppl. Ser. 16, 143.

Linsky, J. L., 1973: "A Recalibration of the Quiet Sun Millimeter Spectrum Based on the Moon as an Absolute Radiometric Standard", Solar Phys. 28, 409.

BIBLIOGRAPHY (Concluded)

Miller, R. H., 1972: "Information-Theoretic Limitations to Optical Object Restoration", in Quarterly Report No. 32, Institute for Computer Research, University of Chicago, Section E.

Raine, W. L., 1970: "A Radiometer for Lunar and Planetary Measurements in the Twenty-Micrometer Window", Summary Report RL-SSL-1215, Teledyne Brown Engineering, Huntsville, Alabama.

Rushforth, C. K., and Harris, R. W., 1968: "Restoration, Resolution and Noise", J. Opt. Soc. Amer. 58, 539.

Shimabukuro, F. I., and Stacey, J. M., 1968: "Brightness Temperature of the Quiet Sun at Centimeter and Millimeter Wavelengths", Astrophys. J. 152, 777.

Ulich, B. L., Cogdell, J. R., and Davis, J. H., 1973: "Planetary Brightness Temperature Measurements at 8.6 mm and 3.1 mm Wavelengths", Icarus 19, 59.

Vernazza, J. E., and Noyes, R. W., 1972: "Inhomogeneous Structure of the Solar Chromosphere from Lyman-Continuum Data", Solar Phys. 22, 358.

Whipple, F. L., 1963: "On the Structure of the Cometary Nucleus", in The Moon, Meteorites, and Comets (ed. B. M. Middlehurst and G. P. Kuiper), University of Chicago Press, Chapter 19.

Zheleznyakov, V. V., 1964: "Model of the Lower Chromosphere Based on Radio Data", Astronomicheskii Zhurnal 41, 1021; translated in Soviet Astronomy-AJ 8, 819 (1965).